PHOTON 2019 - International Conference on the Structure and the Interactions of the Photon

3-7 June 2019

INFN - LNF, Frascati

Satellite Workshop:
Photon Physics and Simulation at Hadron Colliders
6-7 June 2019

Recent results on two photon processes at BaBar

Peter A. Lukin

Budker Institute of Nuclear Physics and

Novosibirsk State University

on behalf of BaBar Collaboration

Novosibirsk State University
*THE REAL SCIENCE

Outline

- Introduction
- Collider and Detector
- Two photon processes at BaBar
- Summary

Introduction. Classification of $\gamma\gamma$ Experiments

There are three different types of $\gamma\gamma$ experiments depending on whether or not initial electrons are detected:

- Both $e^{\pm}$ not detected – no tag (small $q^2_{1,2}$, quasireal photons)
- One $e^{\pm}$ is detected – single tag
- Both $e^{\pm}$ detected – double tag

In some cases experiments have a dedicated tagging system (tagger) to detect outgoing $e^{\pm}$'s (TPC-2γ, MD-1 in the past, KEDR in Novosibirsk, KLOE-2 in Frascati - today)

Detectors with a large solid angle (CLEO, BaBar, Belle, BES-III) can perform single-tag experiments, when one final lepton is detected

Introduction. Transition FormFactor

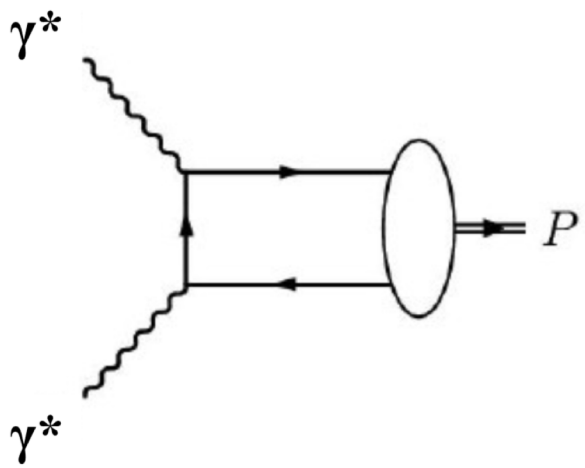

The amplitude of the $\gamma^*\gamma^* \to P$ transition

$$A = e^2 \varepsilon_{\mu\nu\alpha\beta} e_1^\mu e_2^\nu q_1^\alpha q_2^\beta F(q_1^2, q_2^2),$$

P — pseudoscalar meson
$e_{1,2}$ — photon polarization
$q_{1,2}$ — 4-momentum of photon

- there are a lot of experimental study of pseudoscalar meson production via the fusion of real (**on-shell**) and virtual (**off-shell**) photons

$\gamma^*\gamma \to P$: π^0, η, η', η_c

- there are **no** measurements of the double **off-shell** transitions

$\gamma^*\gamma^* \to P$

Introduction. $F(Q^2_1,Q^2_2)$ at large Q^2

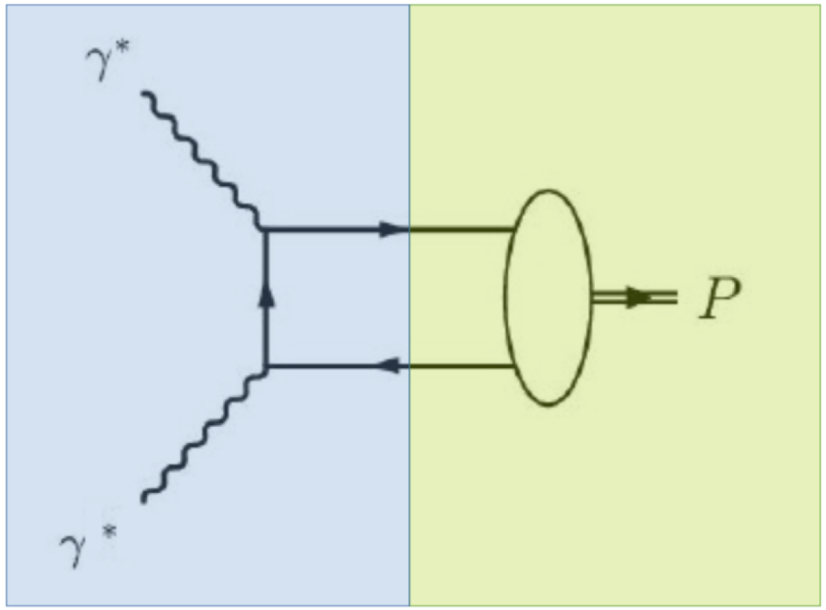

Hard part *Warm part*

$$\mathbf{F(Q^2_1,Q^2_2) = \int T(x,Q^2_1,Q^2_2)\, \varphi(x,Q^2_1,Q^2_2)\, dx}$$

x - is the fraction of the meson momentum carried by one of the quarks

$T(x,Q^2_1,Q^2_2)$ - hard scattering amplitude for $\gamma^*\gamma^* \to$ qqbar transition which is calculable in pQCD

$\varphi(x,Q^2_1,Q^2_2)$ - nonperturbative meson distribution amplitude (DA) describing transition P → qqbar

$$T_H(x,Q_1^2,Q_2^2) = \frac{1}{2}\cdot\frac{1}{xQ_1^2+(1-x)Q_2^2}\cdot\left(1+C_F\frac{\alpha_S(Q^2)}{2\pi}\cdot t(x,Q_1^2,Q_2^2)\right)+(x\to 1-x)+\mathcal{O}(\alpha_S^2)+\mathcal{O}(\Lambda_{QCD}^4/Q^4)$$

NLO Correction [E. Braaten, Phys. Rev. D **28**, 3 (1983)]

- The meson DA **$\varphi(x,Q^2_1,Q^2_2)$** plays an important role in theoretical descriptions of many QCD processes. Its shape (x dependence) is unknown, but its evolution with **$\mu^2 = Q^2_1+Q^2_2$** is predicted by pQCD:

$$\mu^2\frac{d}{\mu^2}\varphi(x,\mu) = \frac{\alpha_S(\mu)}{2\pi}\int_0^1 dy V(x,y)\varphi(y,\mu)$$

At the limit **$\mu\to\infty$** $\varphi_P(x,\mu) = A_P 6x(1-x)(1+O(\Lambda^2_{QCD}/\mu^2))$

S. J. Brodsky and G. P. Lepage, Phys. Rev. D 24, 7 (1981)]

Introduction. $F(Q^2_1,Q^2_2)$ at low Q^2

- F(0,0) is related to axial anomaly:

$$\Gamma_{\eta'\to 2\gamma} = \frac{\pi\alpha^2 m^3_{\eta'}}{4}|F(0,0)|^2 = 4.30 \pm 0.16 \text{ keV} \quad \Rightarrow \quad F(0,0) = 0.342 \pm 0.006 \text{ GeV}^{-1}.$$

- The vector meson dominance model is commonly used to describe TFF at low Q^2:

$$F_{\eta'}(Q^2_1, Q^2_2) = \frac{F_{\eta'}(0,0)}{(1+Q^2_1/\Lambda^2_P)(1+Q^2_2/\Lambda^2_P)}$$

- In case of the TFF with one off-shell photon the pQCD and VMD models leads to the same asymptotic behaviour $F(Q^2) \propto 1/Q^2$ at $Q^2 \to \infty$.

	VMD	pQCD
$Q_1^2 \approx 0, Q_2^2 \to \infty$	$1/Q^2$	$1/Q^2$
$Q_1^2, Q_2^2 \to \infty$	$1/Q^4$	$1/Q^2$

A.V. Radyushkin, R. Ruskov, Nuclear Physics B481 (1996) 625-680

$$F^{LO}_{\gamma^*\gamma^*\pi^0}(q^2, Q^2) = \frac{4\pi}{3} \int_0^1 \frac{\varphi_\pi(x)}{xQ^2 + \bar{x}q^2}\, dx, \qquad (1.1)$$

where $\varphi_\pi(x)$ is the pion distribution amplitude and $x, \bar{x} \equiv 1 - x$ are the fractions of the pion light-cone momentum carried by the quarks. In the region where both photon virtualities are large: $q^2 \sim Q^2 \gtrsim 1$ GeV^2, the pQCD predicts the overall $1/Q^2$ fall-off of the form factor, which differs from the naive vector meson dominance expectation $F_{\gamma^*\gamma^*\pi^0}(q^2, Q^2) \sim 1/q^2Q^2 \sim 1/Q^4$. Thus, establishing the $1/Q^2$ power law in this region is a crucial test of pQCD for this process. The study of $F_{\gamma^*\gamma^*\pi^0}(q^2, Q^2)$ over a wide range of the ratio q^2/Q^2 of two large photon virtualities can then provide non-trivial information about the shape of $\varphi_\pi(x)$.

Introduction. $F(Q^2_1,Q^2_2)$ at large Q^2

Master Formula

The meson DA

$$F_{\eta'}(Q_1^2,Q_2^2)=\left(\frac{5\sqrt{2}}{9}f_n\sin\phi+\frac{2}{9}f_s\cos\phi\right)\int_0^1 dx\,\frac{1}{2}\cdot\frac{6x(1-x)}{xQ_1^2+(1-x)Q_2^2}\cdot\left(1+C_F\frac{\alpha_S(Q^2)}{2\pi}\cdot t(x,Q_1^2,Q_2^2)\right)+(x\to 1-x)$$

NLO Correction

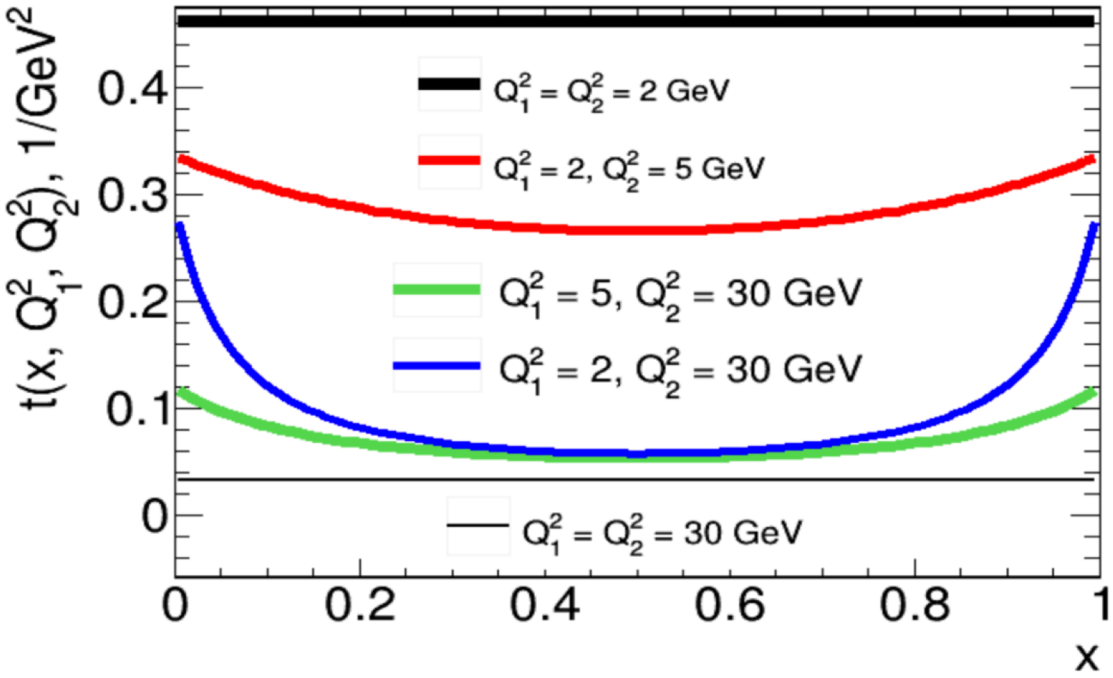

1. The double-virtual transition FF is less sensitive to NLO than the single-virtual one.

2. The form $1/[xQ_1^2+(1-x)Q_2^2]$ is not divergent, so double-virtual transition FF is less sensitive to a shape of the meson DA than the single-virtual FF.

Summary of TFF results

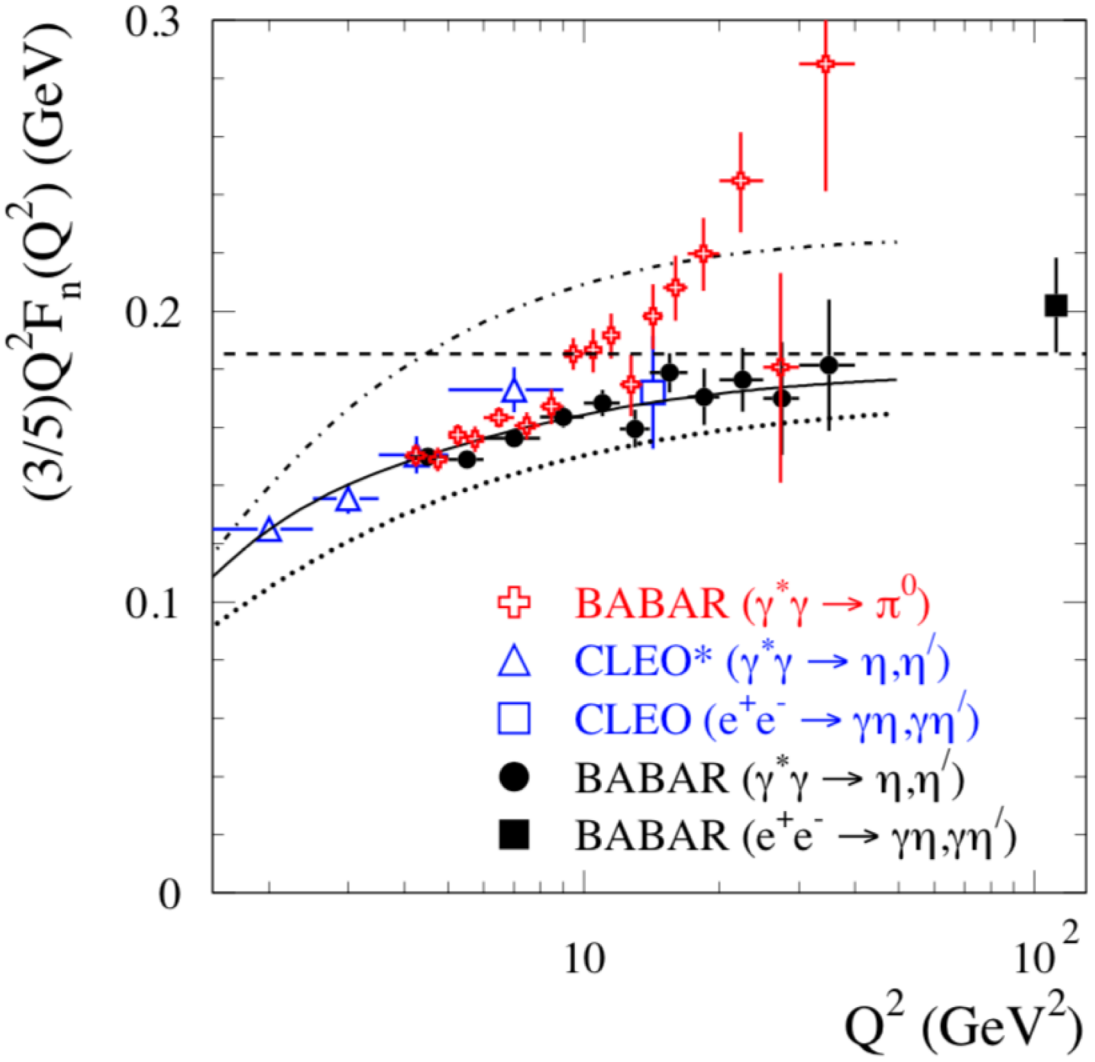

Analysis overview

The analysis is based on the previous BaBar study

previous

Phys. Rev. D 84, 052001 (2011)

γγ*→η'
Single tagged
~ 5000 signal events

new

Phys. Rev. D98, 112002 (2018)

γ*γ*→η'
Double tagged
46^{+8}_{-7} signal events

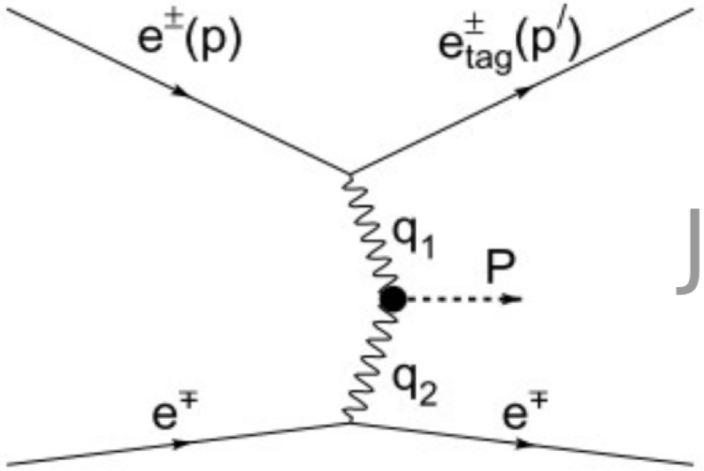

$J^{PC} = 0^{-+}$

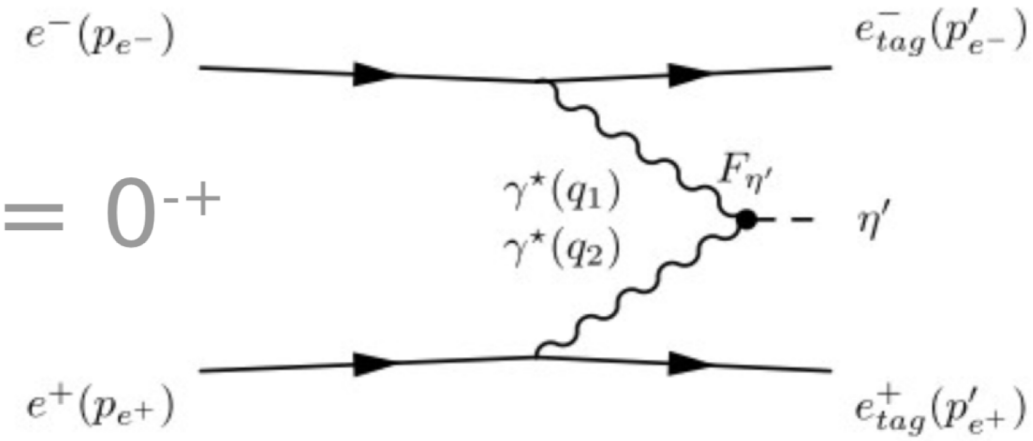

- **A large number of systematic uncertainties were studied in our previous work where the number of signal events was significantly larger.**

BaBar Experiment (1999-2008)

PEP-II: e^+e^- collider, 3.1×9 GeV^2

$\sqrt{s} = 10.58$ GeV $[\Upsilon(4S)]$

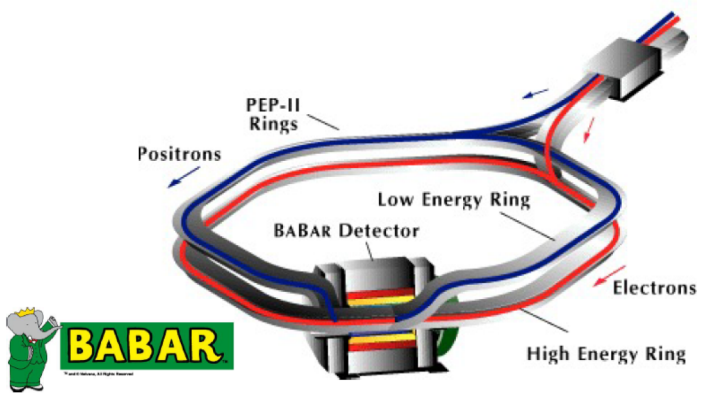

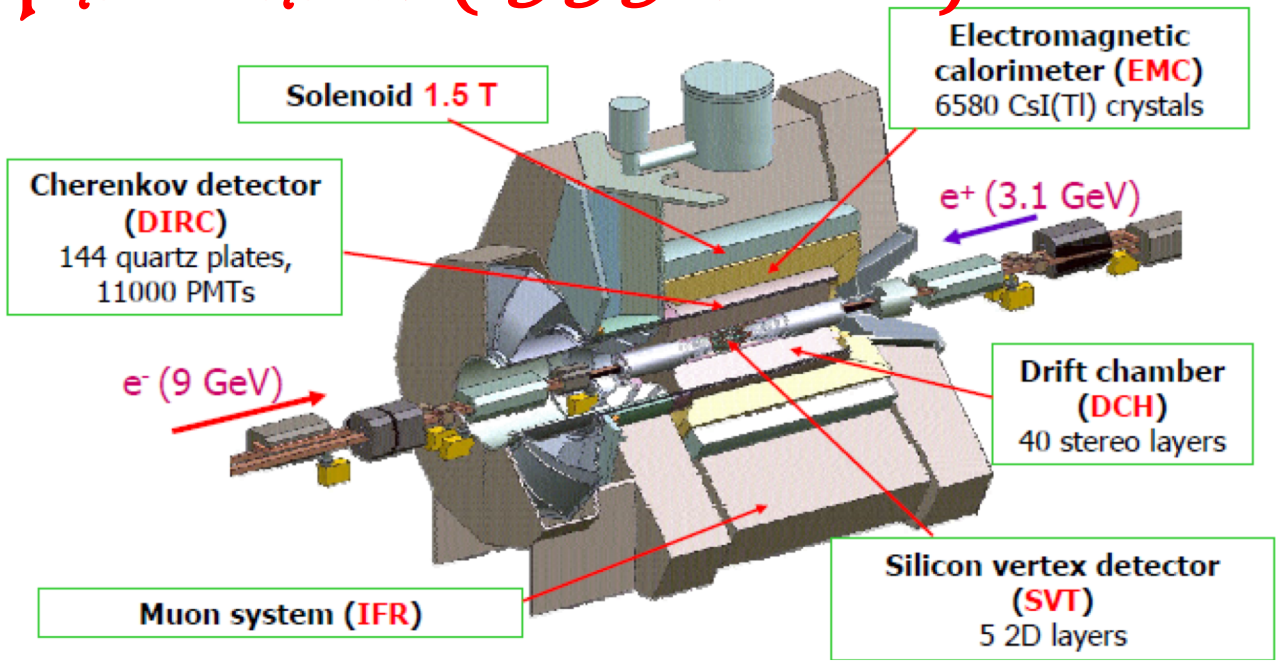

$\mathcal{L}_{peak}$=12.069x10^{33} cm^{-2}s^{-1}

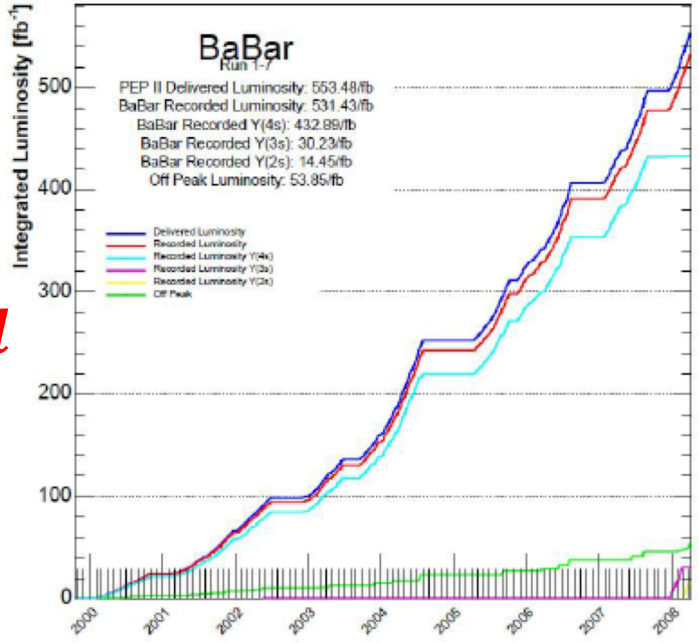

- $\int \mathcal{L}dt \approx 430\ fb^{-1}$@ $\Upsilon(4S)$ *and* $45\ fb^{-1}$ *40 MeV below* $\Upsilon(4S)$
- **470 M BB pairs**
- **Total** $\int \mathcal{L}dt \approx 550\ fb^{-1}$

Technique.

$$q^2_{e^-} = -Q^2_{e^-} = (p_{e^-} - p'_{e^-})^2$$

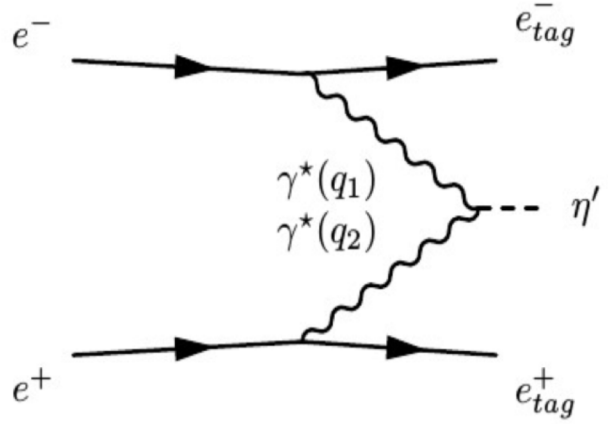

$$q^2_{e^+} = -Q^2_{e^+} = (p_{e^+} - p'_{e^+})^2$$

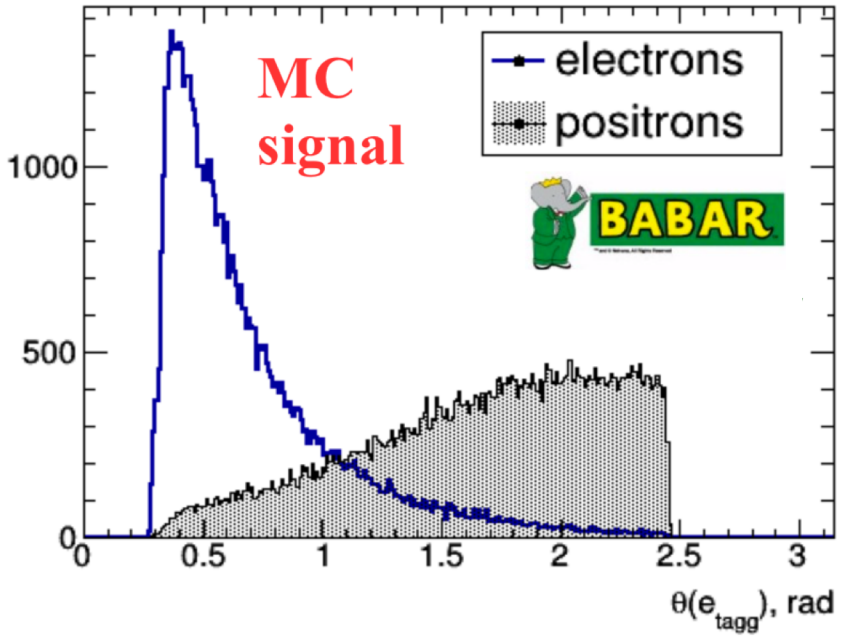

Polar angle distribution for tagged electrons (positrons)

- The decay chain $\eta' \to \pi^+\pi^-\eta \to \pi^+\pi^-2\gamma$ is used
- A total integrated luminosity L = 469 fb^{-1}
- GGResRc event generator is used [arXiv:1010.5969]. Initial and final state radiative corrections as well as vacuum polarization effects are included. The form factor is fixed to the constant value F(0,0).

The strategy: $dN/dQ^2 \Rightarrow d\sigma/dQ^2 \Rightarrow |F(Q^2)|$

Event Selection (I).

• The total reconstructed **momentum** of $e^+e^-\pi^+\pi^-\eta$ system in c.m. frame is less than 0.35 GeV/c.

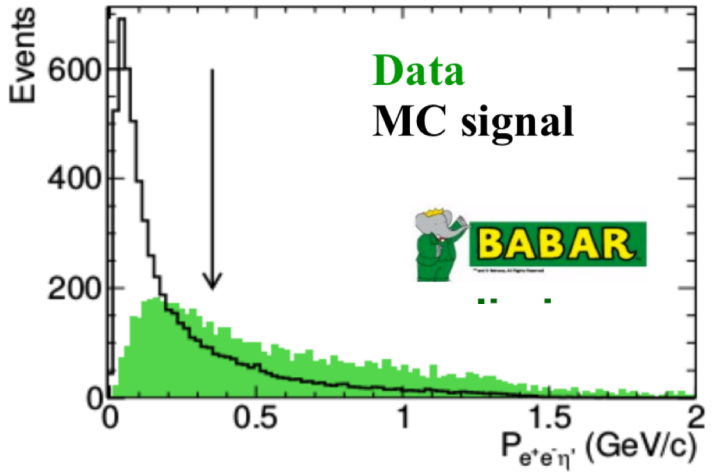

• The total reconstructed **energy** of $e^+e^-\pi^+\pi^-\eta$ system in c.m. frame belongs to the range [10.3:10.7] GeV

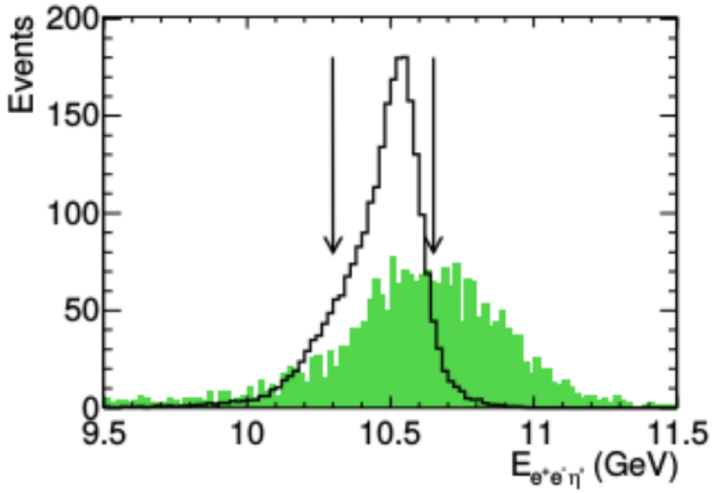

• Events that lie above and on the right of the lines (mostly, Bhabha scattering) are rejected.

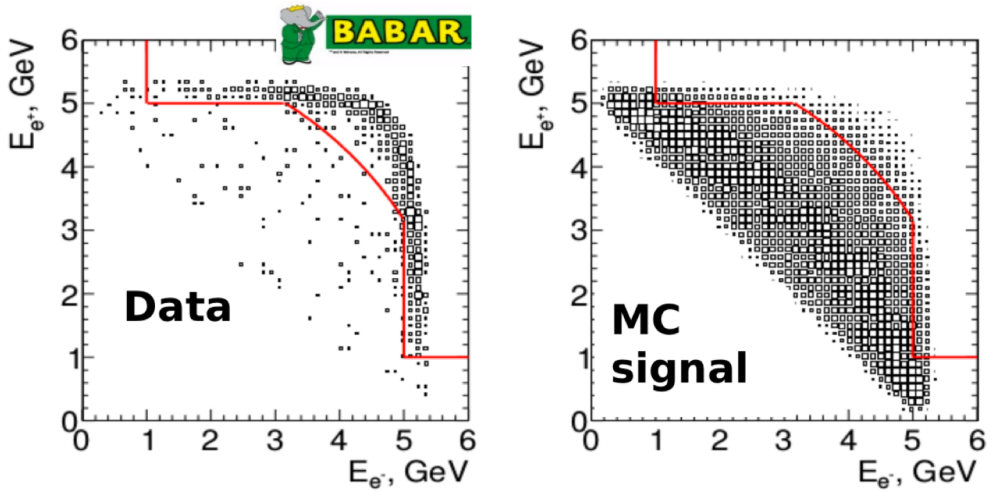

The positron c.m. energy vs. the electron c.m. energy

Event Selection (II).

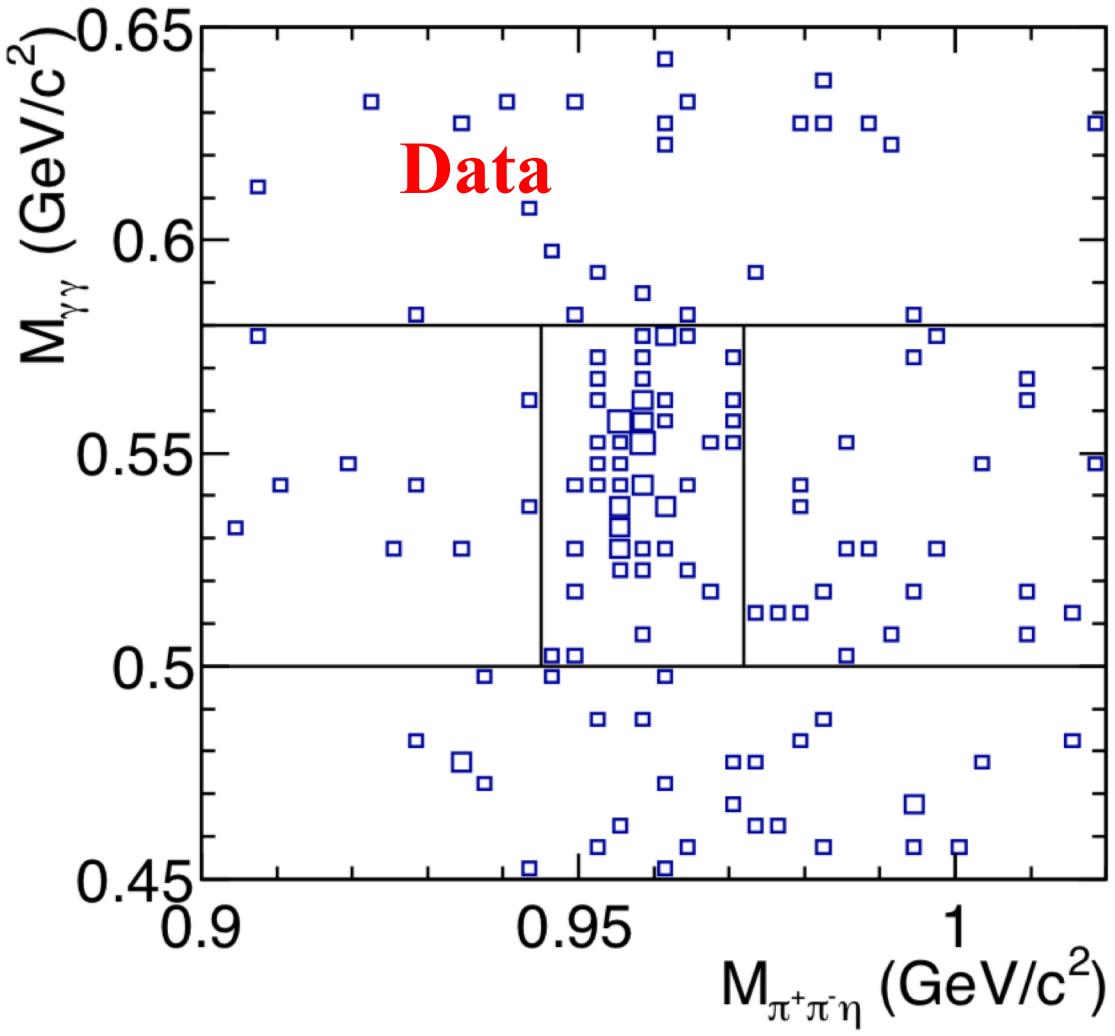

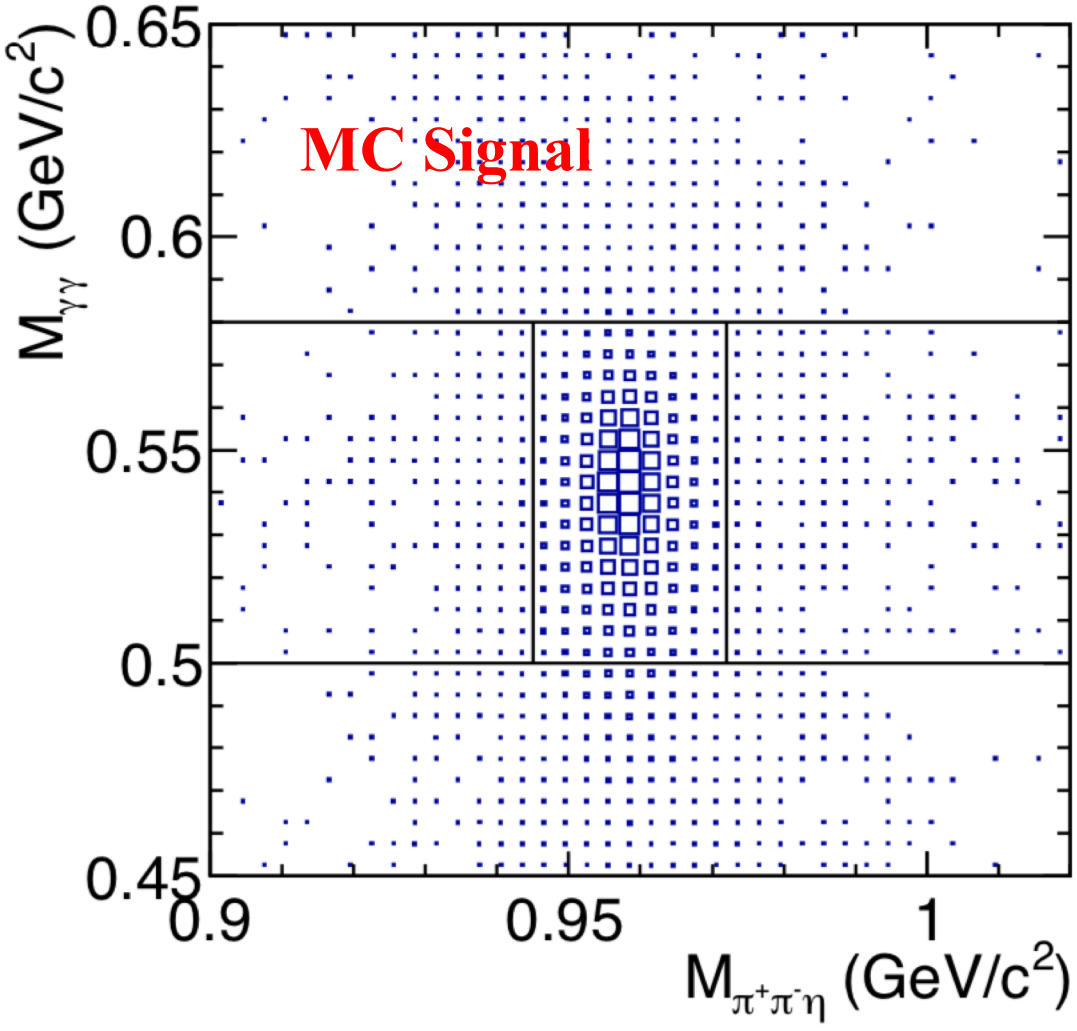

Event Selection (IV).

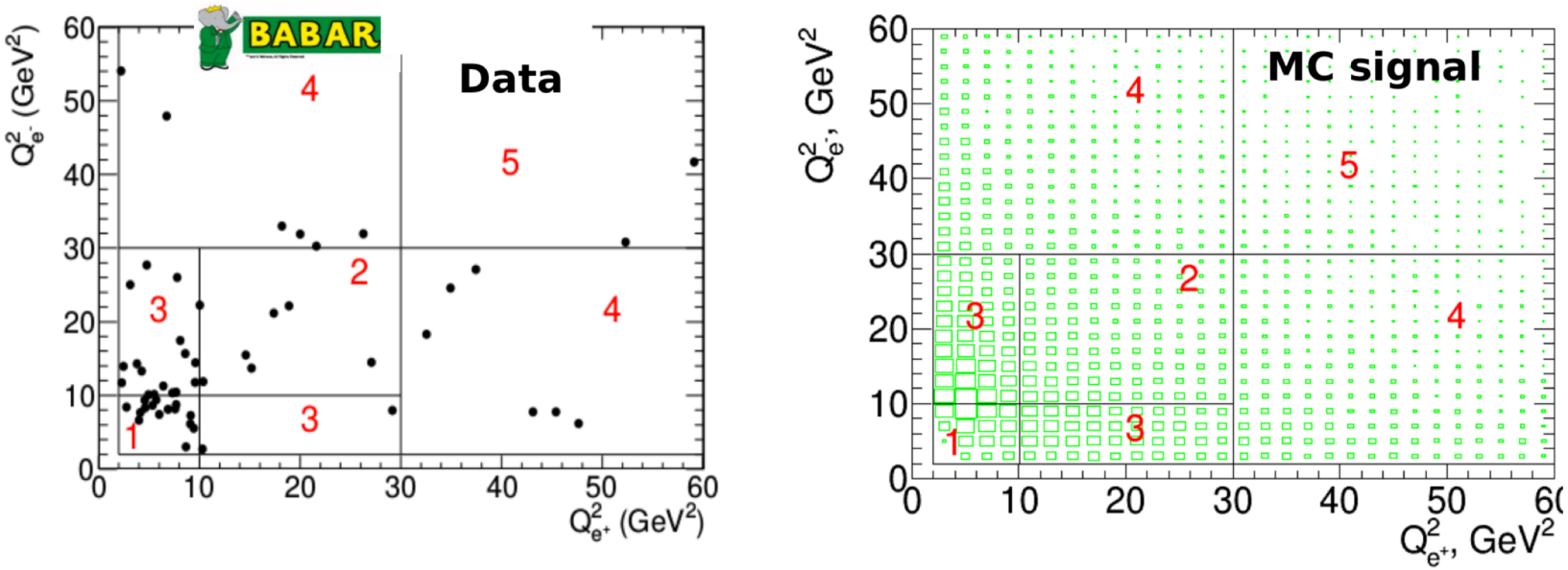

The Q^2_{e-} vs. Q^2_{e+} for events with ***$0.945 < m_{2\pi\eta} < 0.972$*** *GeV/c²*

- New definition: $Q_1^2 = \max(Q_{e+}^2, Q_{e-}^2),\ Q_2^2 = \min(Q_{e+}^2, Q_{e-}^2)$

- The average momentum transfers for each region are calculated using the data spectrum normalized to the detection efficiency:

$$\overline{Q_{1,2}^2} = \frac{\sum_i Q_{1,2}^2(i)/\varepsilon(Q_1^2, Q_2^2)}{\sum_i 1/\varepsilon(Q_1^2, Q_2^2)}.$$

Event Selection (V).

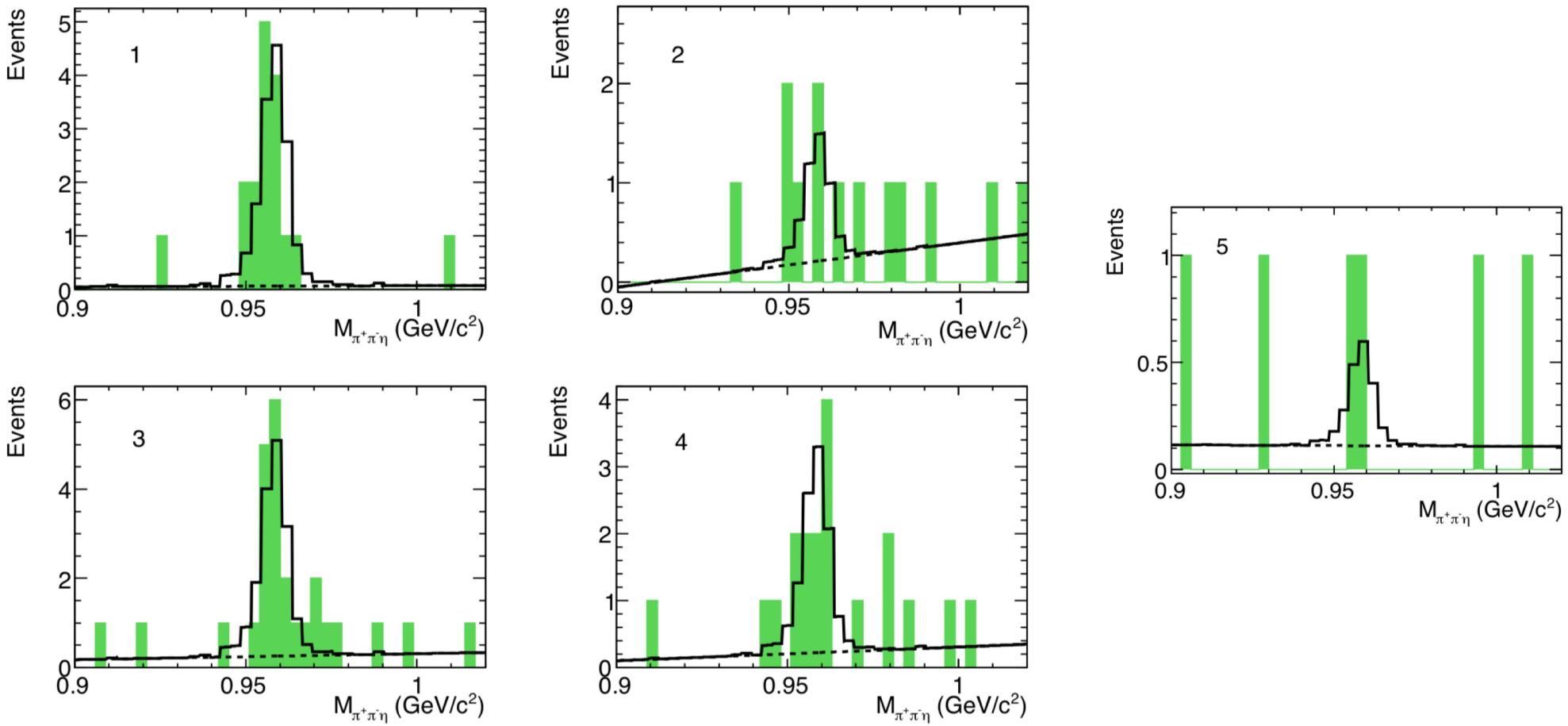

The $\pi^+\pi^-\eta$ mass spectra for data events from the five (Q_1^2, Q_2^2) regions of Fig. 7. The open histograms are the fit results. The dashed lines represent fitted background.

Detection efficiency.

• The detector acceptance limits the e^-e^+ detection efficiency at small Q^2 . The minimum Q^2 equals to 2 GeV^2.

$$\varepsilon_{true} = \frac{\int \varepsilon(Q_1^2, Q_2^2) F_{\eta'}^2(Q_1^2, Q_2^2) dQ_1^2 dQ_2^2}{\int F_{\eta'}^2(Q_1^2, Q_2^2) dQ_1^2 dQ_2^2}$$

F_η, from master formula at Slide #8

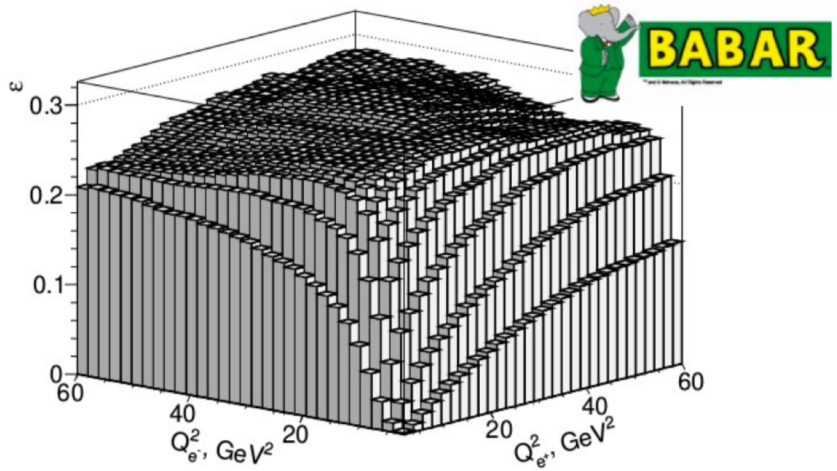

The dependence of detection efficiency on momentum transfers.

• Radiative corrections $R(Q_1^2, Q_2^2) = \frac{\sigma^{rad}(Q_1^2, Q_2^2)}{\sigma^{born}(Q_1^2, Q_2^2)}$

• R leads to the decrease of the detection efficiency by ~ 15 %.

• The maximum energy of the photon emitted from the initial state is restricted by the requirement $E_\gamma < 0.05\sqrt{s}$, where $\sqrt{s}$ is the e^+e^- center-of-mass (c.m.) energy.

Cross section and FormFactor.

- The differential cross section for $e^+e^- \to e^+e^-\eta'$ is calculated as

$$\frac{d^2\sigma}{dQ_1^2 dQ_2^2} = \frac{1}{\varepsilon_{\text{true}} RLB} \frac{d^2N}{dQ_1^2 dQ_2^2}$$

$$F^2(\overline{Q_1^2}, \overline{Q_2^2}) = \frac{(d^2\sigma/(dQ_1^2 dQ_2^2))_{data}}{(d^2\sigma/(dQ_1^2 dQ_2^2))_{MC}} F^2_{\eta'}(\overline{Q_1^2}, \overline{Q_2^2})$$

- $B = B(\eta' \to \pi^+\pi^-\eta) \times B(\eta \to 2\gamma) = (0.3941 \pm 0.0020) \times (0.429 \pm 0.007) = 0.169 \pm 0.003$

- **$\sigma_{e+e-\to e+e-\eta'}$ ($2 < Q_1^2, Q_2^2 < 60$ GeV^2) $= (11.4^{+2.8}_{-2.4})$ fb**

$\overline{Q_1^2}$, $\overline{Q_2^2}$, GeV^2	$\varepsilon_{\text{true}}$	R	N_{events}	$d^2\sigma/(dQ_1^2 dQ_2^2)$ $\times 10^4$, fb/GeV^4	$F(\overline{Q_1^2}, \overline{Q_2^2})$ $\times 10^3$, GeV^{-1}
6.48, 6.48	0.019	1.03	$14.7^{+4.3}_{-3.6}$	$1471.8^{+430.1}_{-362.9}$	$14.32^{+1.95}_{-1.89} \pm 0.83 \pm 0.14$
16.85, 16.85	0.282	1.10	$4.1^{+2.7}_{-2.7}$	$4.2^{+2.8}_{-2.8}$	$5.35^{+1.54}_{-1.54} \pm 0.31 \pm 0.42$
14.83, 4.27	0.145	1.07	$15.8^{+4.8}_{-4.0}$	$39.7^{+12.0}_{-10.2}$	$8.24^{+1.16}_{-1.13} \pm 0.48 \pm 0.65$
38.11, 14.95	0.226	1.11	$10.0^{+3.9}_{-3.2}$	$3.0^{+1.2}_{-1.0}$	$6.07^{+1.09}_{-1.07} \pm 0.35 \pm 1.21$
45.63, 45.63	0.293	1.22	$1.6^{+1.8}_{-1.1}$	$0.6^{+0.7}_{-0.6}$	$8.71^{+3.96}_{-8.71} \pm 0.50 \pm 1.04$

Statistical uncertainty is dominated

Statistical **Systematic** **Model**

Summary

- About 46 events of $e^+e^- \longrightarrow e^+e^-\eta'$ were observed in the double tagged mode for the first time

- The $\gamma^*\gamma^* \longrightarrow \eta'$ transition formfactor $F(Q^2_1,Q^2_2)$ has been measured for Q^2 range from 2 to 60 GeV^2.

- The formfactor is in reasonable agreement with the pQCD prediction and contradicts the prediction of VDM

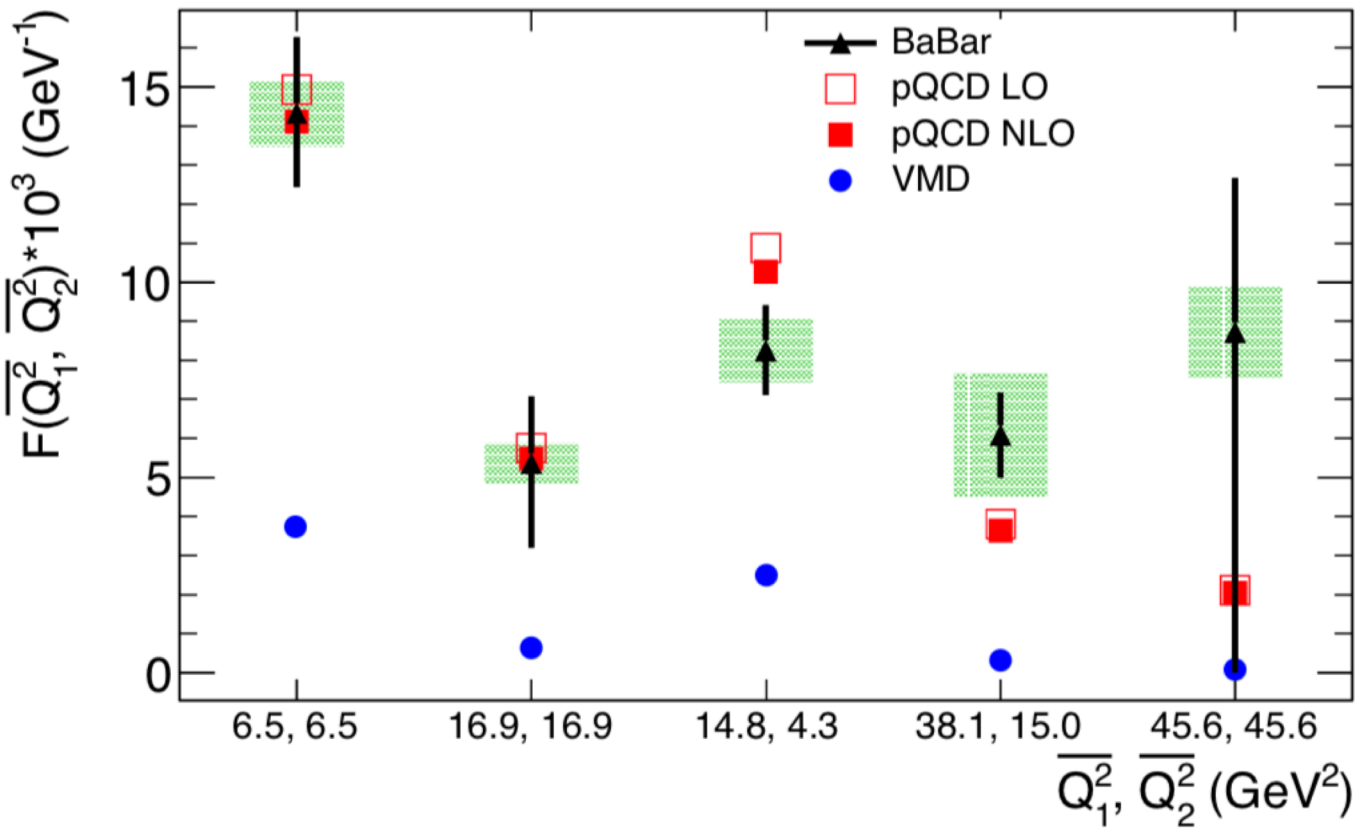

Spare Slides

Introduction. Basic features of $\gamma\gamma$ collisions

- $\sigma(e^+e^- \to e^+e^-\gamma^*\gamma^* \to e^+e^- f) \propto \alpha^4 log^2 E/m_e$
  compared to
  $\sigma(e^+e^- \to \gamma^* \to f) \propto \alpha^2/E^2$

- Particles produced in $\gamma\gamma$ collisions have $C = +1$ and $J^P = 0^\mp, 2^\mp$ while those in single-photon annihilation have $C = -1$ and $J^P = 1^-$

- Special kinematics:
  - Initial electrons tend to fly in their original directions and lose a small part of their energy
  - The produced system of particles f has $E_{\rm tot} \ll \sqrt{s} = 2E$ and tends to have small transverse momentum

Event Selection (III).

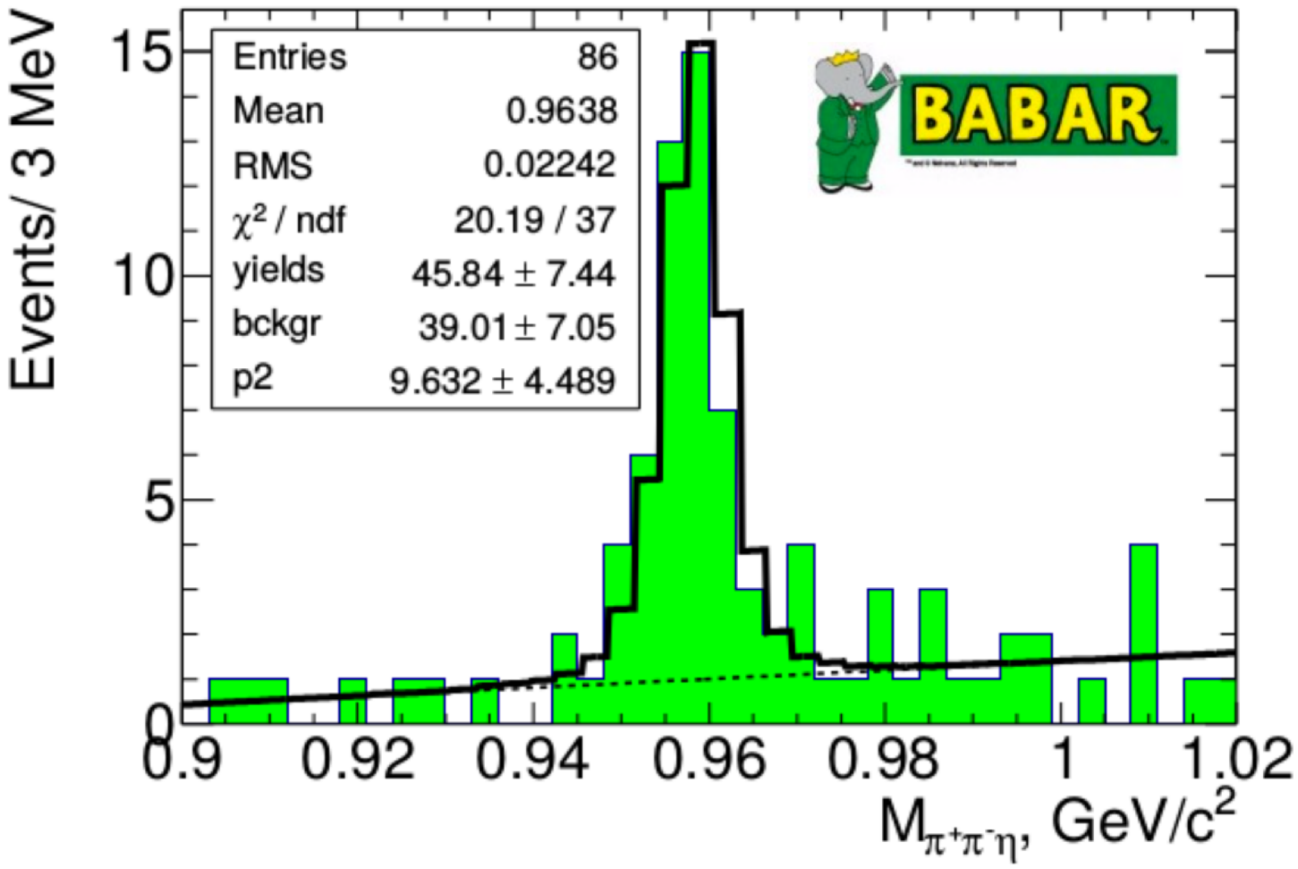

The $\pi^+\pi^-\eta$ mass spectra for data events. The open histogram is the fit result. The dashed line represents fitted background.